

CaDM: Codec-aware Diffusion Modeling for Neural-enhanced Video Streaming

Qihua Zhou, Ruibin Li, Song Guo, Yi Liu, Jingcai Guo, Zhenda Xu
Department of Computing, The Hong Kong Polytechnic University

{qi-hua.zhou, ruibin.li, joeylau.liu, jackal.xu}@connect.polyu.hk
{song.guo, jc-jingcai.guo}@polyu.edu.hk

Abstract

Recent years have witnessed the dramatic growth of Internet video traffic, where the video bitstreams are often compressed and delivered in low quality to fit the streamer's uplink bandwidth. To alleviate the quality degradation, it comes the rise of Neural-enhanced Video Streaming (NVS), which shows great prospects to recover low-quality videos by mostly deploying neural super-resolution (SR) on the media server. Despite its benefit, we reveal that current mainstream works with SR enhancement have not achieved the desired rate-distortion trade-off between bitrate saving and quality restoration, due to: (1) overemphasizing the enhancement on the decoder side while omitting the co-design of encoder, (2) inherent limited restoration capacity to generate high-fidelity perceptual details, and (3) optimizing the compression-and-restoration pipeline from the resolution perspective solely, without considering color bit-depth. Aiming at overcoming these limitations, we are the first to conduct the encoder-decoder (i.e., codec) synergy by leveraging the visual-synthesis genius of diffusion models. Specifically, we present the Codec-aware Diffusion Modeling (CaDM), a novel NVS paradigm to significantly reduce streaming delivery bitrate while holding pretty higher restoration capacity over existing methods. First, CaDM improves the encoder's compression efficiency by simultaneously reducing resolution and color bit-depth of video frames. Second, CaDM provides the decoder with perfect quality enhancement by making the denoising diffusion restoration aware of encoder's resolution-color conditions. Evaluation on public cloud services with OpenMMLab benchmarks shows that CaDM significantly saves streaming bitrate by a nearly 100 \times reduction over vanilla H.264 and achieves much better recovery quality (e.g., FID of 0.61) over state-of-the-art neural-enhancing methods.

1. Introduction

The video traffic has experienced tremendous growth with the emergence of Internet streaming services (e.g.,

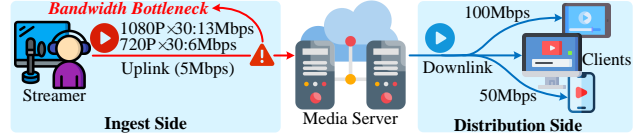


Figure 1. Overview of a common video streaming infrastructure.

Zoom meeting [73] and YouTube live [66]) over the last decade. As shown in Figure. 1, today's video streaming infrastructure usually consists of two sides: (1) the ingest side where the streamer uploads video bitstreams to the media server through the streamer's uplink [10, 25, 37, 60], and (2) the distribution side where the server broadcasts the prepared videos to clients through the server's downlink [20, 29, 33, 41]. The ingest side often requires low-latency streaming protocols for video delivery [19, 24, 45, 47] and the distribution side involves the deployment of adaptive bitrate (ABR) algorithms [40, 41, 56, 58] to match client's Quality of Experience (QoE) [1, 62, 65, 68].

Unfortunately, a practical issue is that the streamer's uplink bandwidth is usually far lower than the server's downstream bandwidth [9, 38, 68], making the ingest side become the performance bottleneck for continuously delivering high-definition videos [14, 31, 63]. To fit the limited uplink bandwidth, a natural methodology is to compress the video bitstreams in low quality for realizing communication-efficient delivery, e.g., from 1080P/720P to 360P. The frame compression usually involves two key perspectives: (1) the downscaling of spatial resolution [21, 23, 27, 72] and (2) the reduction of color bit-depth to represent a pixel [30, 32, 35, 69]. Obviously, compression from either perspective will deprive the server from obtaining high-quality videos and finally hampers the perceptual experience of downstream distribution services, especially when video quality often significantly impacts user's engagement in video streaming [11, 13, 26, 51, 71]. To alleviate the performance bottleneck on the ingest side in current video streaming infrastructure, it comes the rise of *Neural-enhance Video Streaming* (NVS) paradigm [9, 14, 22, 31, 61, 63], where a majority of works aim to restore the compressed video quality by deploying a neural super-resolution (SR) model on the media

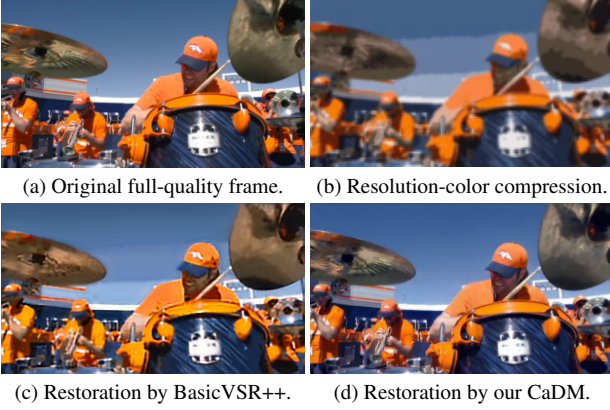


Figure 2. Visualization of neural-enhanced video streaming in different stages: (a) the original full-quality frame, (b) encoder’s resolution-color compression, (c) decoder’s restoration by SOTA BasicVSR++ [4], and (d) decoder’s restoration by our CaDM that achieving pretty higher enhancement quality over BasicVSR++.

server [22, 38, 55, 61, 63, 68]. The restored videos should hold sufficient visual quality as the original version, so as to guarantee the service experience of downstream video distribution. Consequently, the core objective of NVS is to reduce the delivery bitrate while restricting the quality distortion of restored videos in an acceptable range.

However, our preliminary experiments verified that current mainstream works with SR enhancement have not achieved a desired *rate-distortion* trade-off between bitrate saving and quality restoration. As illustrated in Figure. 2, we visualize the original, compressed and restored frames in the NVS pipeline. It is clear that even adopting state-of-the-art (SOTA) BasicVSR++ method [4] cannot guarantee a desired quality restoration when the frame is compressed with low spatial resolution and color bit-depth. We reveal that existing SR-based NVS methods fall short of restoring low-quality frames due to: (1) overemphasizing the enhancement on the decoder side while omitting the co-design of encoder, (2) inherent limited restoration capacity to generate high-fidelity perceptual details, and (3) optimizing the compression-and-enhancement pipeline from the resolution perspective solely, without considering color bit-depth.

These limitations motivate us to improve the encoder-decoder (*i.e.*, codec) synergy and design a new NVS paradigm to significantly reduce delivery bitrate while providing a much higher restoration capacity over existing methods. To achieve this target, we present the *Codec-aware Diffusion Modeling* (CaDM), which perfectly restores the low-quality videos by leveraging the visual-synthesis genius of diffusion models. First, CaDM improves the encoder’s compression efficiency by simultaneously reducing resolution and color bit-depth of video frames (§3.2). Second, CaDM provides the decoder with powerful quality enhancement by making the denoising dif-

fusion restoration aware of encoder’s resolution-color conditions (§3.3). Extensive experiments on public cloud services with OpenMMLab benchmarks show that CaDM significantly saves delivery bitrate by a nearly 100× reduction over vanilla H.264 [15] and achieves the highest recovery quality over state-of-the-art neural-enhancing methods.

In summary, our key contributions are as follows.

- **Novel NVS paradigm.** To the best of our knowledge, CaDM is the first work to essentially solve the key bottleneck on the ingest side of video streaming infrastructure. It conducts an encoder-decoder synergy (§3.1) to significantly improve the *rate-distortion* trade-off against current NVS paradigm.
- **Tremendous compression ratio.** CaDM effectively fits the streamer’s uplink capacity and significantly reduces the video delivery bitrate by an order of magnitude. It improves the encoder’s compression efficiency by simultaneously downscaling the spatial resolution (§3.2.1) and reducing the color bit-depth (§3.2.2).
- **State-of-the-art restoration performance.** CaDM leverages the visual-synthesis genius of diffusion models to perfectly improve decoder’s enhancement capacity (§3.3), achieving state-of-the-art restoration performance in different quality assessment metrics (§4.2).

2. Related Work

2.1. Video Streaming Infrastructure

With the unprecedented boom of video perception services (*e.g.*, Zoom meeting [73] and YouTube live [66]), video streaming has become a significant information carrier for today’s Internet. As shown in Figure. 1, current video streaming infrastructure is usually composed of the ingest and distribution side [22, 61, 63]. On the ingest side, the streamer (*e.g.*, a YouTuber) creates videos and uploads the encoded bitstreams to the media server. The server receives the bitstreams, decodes them, and stores the videos for subsequent distribution tasks. On the distribution side, the media server broadcasts the prepared videos to all clients (*e.g.*, the YouTube subscribers). Consistent with recent mainstream works [14, 31, 63], this paper focuses on the video streaming performance on the ingest side, *i.e.*, involving the uplink from the streamer to the server. A practical issue is that the streamer’s uplink bandwidth is usually far lower than the server’s downlink bandwidth [9, 38, 68]. As a result, the streamer has to compress the video bitstreams in low quality to save the delivery bitrate. This issue hampers the server from obtaining high-quality videos.

2.2. Neural-enhanced Video Streaming

To eliminate the limitation of ingest side in traditional video streaming infrastructure, it comes the *Neural-enhanced Video Streaming* (NVS) [9, 14, 22, 31, 61, 63]

paradigm. To improve the delivery performance on the ingest side, NVS involves the collaboration between streamer and server. First, the streamer downscales the original high-resolution video frames into the low-resolution version, then encodes the frames into video bitstreams for network transmission. The media server decodes the bitstreams as a series of frames and fed them into a neural super-resolution (SR) model for quality enhancement [22, 38, 61, 63, 68]. The final restored video holds comparable visual experience as the original version, thus can be applied to the content distribution in different downstream tasks. Recently, optimizing the NVS pipeline has become a hot topic, including improving video encoding efficiency [9, 14], reducing streaming protocol latency [62], designing adaptive bit-rate delivery [9] and optimizing SR enhancement [38, 59, 67]. Overall, the core objective of an efficient NVS paradigm is to improve the *rate-distortion* trade-off for video delivery, *i.e.*, reducing the streaming bitrate while restricting the quality drop of restored videos.

2.3. Neural-enhancing Models

Restoring the compressed videos with high-fidelity visual details is a fundamental component of NVS paradigm. Current mainstream NVS frameworks often employ a neural super-resolution (SR) model for quality enhancement. Modern SR techniques mainly exploit the power of deep neural networks, aiming at transferring the low-resolution image to high-resolution version, *e.g.*, EDSR [27], EUSR [6] and FRSR [48]. As the video consists of a series of frames, the SR model can also be applied to enhance video quality, *e.g.*, IconVSR [3], RealBasicVSR [5] and BasicVSR++ [4]. Some modern video SR models also leverage the generative networks to compensate spatial-temporal coherence across frames, *e.g.*, TecoGAN [8], PULSE [36] and Real-ESRGAN [52]. Recently, the diffusion probabilistic models (*e.g.*, DDPM [17], DDIM [49] and LDM [42]) have achieved impressive performance in diverse generative tasks, including inpainting [34], colorization [50] and image synthesis [43]. Inspired by the latest research progress of neural-enhancing models, we intend to conduct the encoder-decoder (*i.e.*, codec) synergy by leveraging the visual-synthesis genius of diffusion models. We present the *Codec-aware Diffusion Modeling* (CaDM, §3), a novel NVS paradigm to significantly improve the *rate-distortion* trade-off over SOTA methods.

3. Codec-aware Diffusion Modeling

3.1. Problem Formulation and Objective

Traditional video streaming. As a video consists of a series of frames \mathbf{x} , we use x_i to denote an original raw high-quality frame with index i , where $x_i \in \mathbf{x}$ and i identifies the sequence order for video encoding. After encoding

all the frames as a high-quality video, the video bitstreams will be delivered through the network to the ingest server. The server receives the bitstreams and decodes it for downstream tasks. We can adopt the standard H.264 [15] protocol to handle the entire encoder-decoder procedure and formulate the traditional video streaming pipeline $f(\cdot)$ as:

$$f(\mathbf{x}) = \text{Decode}(\text{Encode}(\mathbf{x})). \quad (1)$$

Neural-enhanced video streaming. Recent NVS researches [9, 14, 22, 61, 63] have shown that directly encoding the video from raw frames and delivering the high-quality video through network is impractical due to streamer’s limited uplink bandwidth. Conducting frame compression before video encoding is necessary to fit the bandwidth restriction, where downscaling the frame resolution with a constant scaling factor (*e.g.*, from 1920×1080 pixels to 480×270 pixels with a $4\times$ factor) is the mainstream methodology [22, 38, 61, 63, 68]. As a result, practical NVS frameworks usually encode a low-resolution video based on the down-scaled frames, deliver the video bitstreams through the network, and decode the bitstreams to a series of low-quality frames for subsequent processing. Since the frame quality is degraded, a pre-trained neural super-resolution (SR) model is adopted by the decoder to recover the visual quality. The SR-enhanced decoder transfers the low-resolution frames back to the high-resolution version [38, 63, 68], *e.g.*, upscaling the 480×270 frames to the original 1920×1080 ones. Thus, a typical NVS pipeline can be described as:

$$f(\mathbf{x}) = \text{Decode}(\text{Encode}(\mathbf{x}; s); \text{SR}), \quad (2)$$

where s is the scaling factor used in resolution downscaling and the neural SR model.

Our CaDM paradigm. Different from existing work, we reveal that the color bit-depth, *i.e.*, the number of bits to represent a unique pixel in visual, has not been well exploited to further reduce the frame size. Figure. 3 illustrates the pipeline of our CaDM’s paradigm. By conducting the frame compression from bit-depth and resolution perspectives simultaneously, the encoder can achieve a much higher compression ratio over the existing NVS methods. However, as more visual information has been compressed, we need a more powerful enhancement module to restore the perceptual details. As verified by our preliminary experiments, conventional SR models used by current NVS cannot achieve a desired restoration performance due to inherent limited generative capacity. This motivates us to re-design the neural enhancement by leveraging the visual-synthesis genius of diffusion models. We design the *Codec-aware Diffusion Modeling* (CaDM), a novel NVS paradigm, to achieve this target. Together with the resolution scaling factor s , color bit-depth n , and diffusion model parameters θ , the entire pipeline of our CaDM can be formulated as:

$$f(\mathbf{x}) = \text{Decode}(\text{Encode}(\mathbf{x}; s, n); \theta). \quad (3)$$

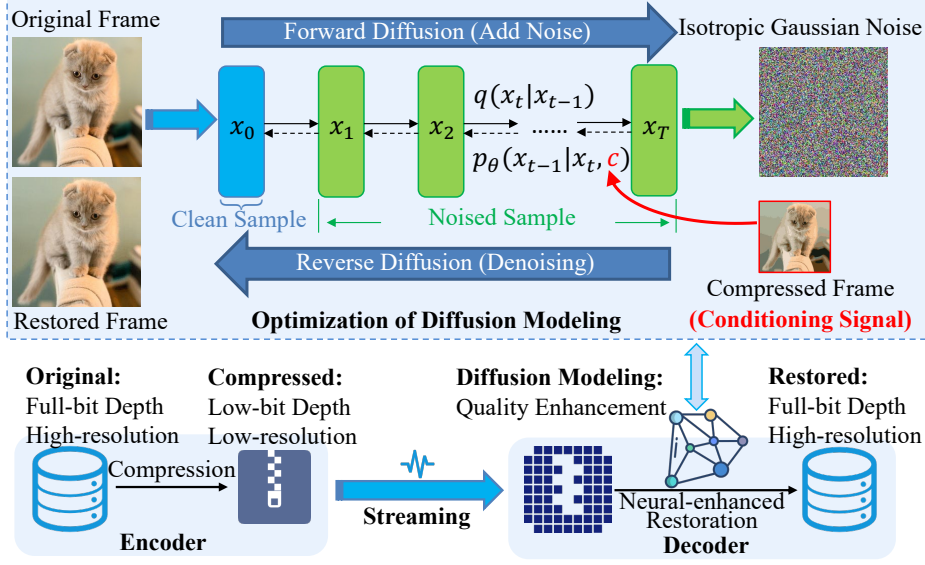


Figure 3. The pipeline of our CaDM paradigm, which restores the low-quality videos by considering frame resolution and color bit depth.

Objective. By embedding the variables of s and n into diffusion conditions (§3.3.1), our objective is to optimize CaDM by training on public video datasets (§3.3.2) to *minimize the gap between restored video frames $f(\mathbf{x})$ and the original ones \mathbf{x}* . We will discuss how CaDM handles the encoder-decoder synergy in the following sections.

3.2. Encoder with Resolution-color Compression

The role of CaDM’s encoder is to reduce the video size with a much higher compression ratio over existing NVS methods, so as to save the delivery bitrate. Note that an extreme compression will lead to a significant degradation on frame visual quality, which may exceed the restoration capacity of the neural-enhancement model on the decoder. We cannot introduce an arbitrary compression mechanism, but need to conduct compression based on the decoder’s restoration property. Thus, we handle the compression from two aspects: (1) downscaling the frame resolution in §3.2.1 and (2) reducing the pixel color bit-depth in §3.2.2.

3.2.1 Patch-wise Resolution Downscaling

The first compression perspective is to downscale the frame resolution, *i.e.*, shrinking the spatial size under the control of a scaling factor s . As the number of pixels within the frame is reduced in both width and height dimensions, resolution downscaling can provide a $s^2 \times$ frame size reduction compared with the original frame. Although fewer pixels are used to represent a frame, its basic visual features should be preserved, otherwise, the visual quality degradation will exceed the decoder’s recovery capacity. This property requires the scaling algorithm to retain the most representative pixels by analyzing the numerical distribution in each

frame patch (*i.e.*, the macroblock, a non-overlapping square block with $s \times s$ pixels in visual). As a preliminary concept to video codec, patch can serve as the basic processing units to explore intra- and inter-frame correlation [9, 22, 61–63]. In default, we suggest using 4×4 patch size, which is a sufficient fine-grained granularity to retain visual features after downscaling. Therefore, as for each pixel, we can figure out a patch where this pixel locates in the center. Specifically, considering the pixels on the frame border, we adopt zero-padding to the border with $\lceil \frac{s}{2} \rceil$ pixels in width and height, so as to guarantee complete patches. Given a scaling factor s , we can divide the frame into a series of $s \times s$ patches. Based on the patch division, we introduce a *Gaussian Blur* to the frame and smooth the features involving a junction of patches. Inside each patch, we calculate the weighted average of all the pixels inside and shrink the patch by this average. Therefore, the entire frame can be downscaled by $s \times$ in both width and height dimensions.

3.2.2 Color Bit-depth Quantization

The second compression perspective is to reduce the color bit-depth, *i.e.*, the number of bits to identify a unique pixel. As to the common H.264 video codec, the source frames are usually organized with 8-bit color space with RGB channels. Therefore, each pixel within a frame is represented in 24 bits, which is similar to the color space of PNG and JPEG formats [30, 32]. We reveal that the pixel vectors along the RGB channel hold similar distributions when they describe close colors in visual. This motivates us to conduct vector quantization to reduce the number of different colors represented by the pixels. For example, if we quantize the color space into 4 bits with 2^4 different colors, the frame

size can be compressed into $4/24$ as the original frame with full-color bit-depth. The key here is to find a proper vector quantization scheme to transfer the full bit-depth pixels into low bit-depth ones. To achieve this target, we introduce the K-means clustering to handle the quantization procedure, which contains the following two steps.

Step #1: Codebook generation. This step aims at generating the quantization codebook that maps all pixels from full color bit-depth to low bit-depth, *e.g.*, from original 24-bit color space to 4-bit version. This requires us to group all the pixels within the frames into several clusters and represent all the pixels belonging to the same cluster by its centroid, so as to reduce the information entropy (reflected by number of bits) to identify each unique pixel. Here, the number of clusters is called the quantization level, which directly impacts the representation precision of the pixel color space. If we adopt n -bit to generate the quantization codebook, all the pixels will be grouped into 2^n clusters. In our CaDM, n is set in range of $[4, 8]$ to greatly reduce frame size over the original 24-bit color space. Given n -bit budget to represent the color space, we choose the K-means clustering to generate the quantization codebook. Note that we need to restrict the computational overhead of calculating K-means clustering model because it iteratively calculates the neighbourhood distance for each pixel. Although we have downscaled the resolution before color quantization, the pixel number of low-resolution frame is still in order of magnitude of $10^5 - 10^6$. In this case, directly adopting K-means on the entire frame pixel is computational unacceptable. To address this challenge, we uniformly sample a subset of pixels (usually in order of magnitude of 10^3) from the frame and obtain K-means clustering model based on these samples. The K-means model describes how to map all the pixels into 2^n clusters and figures out the all cluster centroids. Each centroid is assigned with a unique index, ranging from 0 to $2^n - 1$. Therefore, the gist of our quantization codebook is to map each pixel to its corresponding cluster centroid, which can be represented by n bits.

Step #2: Pixel quantization. Based on the first step of generating quantization codebook, the second step is to replace each pixel by its cluster centroid. The original pixel matrix describing a frame can be transferred as the centroid matrix with the same shape, where each element corresponds to the pixel's centroid. As a result, the original full bit-depth pixels are quantized into n bit-depth version. The frame size is compressed to $\frac{n}{24}$ of the raw frame in 24-bit color space. In realistic deployment, the codebook can be obtained and sent to the ingest server in advance. Therefore, the communication cost for transmitting codebook can be omitted.

Summary. Overall, given the scaling factor s and color bit-depth n , we can figure out the entire compression ratio over traditional 24-bit full-resolution frames as $\frac{24s^2}{n}$.

3.3. Decoder with Denoising Diffusion Restoration

On the streamer side, our CaDM's encoder aims at providing a great compression ratio to reduce video delivery bitrate. Meanwhile, we deploy CaDM's decoder on the ingest server to recover the video bitstreams and enhance the visual quality by leveraging the visual-synthesis genius of diffusion models. As a kind of generative model, we optimize the decoder based on probabilistic theory. The gist of our decoder is to recover the low-quality video bitstreams through a series of denoising steps. Inside each step, we try to minimize the gap between predicted noise and the true noise, which is handled by a pre-trained diffusion model. The diffusion model is established with two key concepts: (1) distortion-aware conditioning (§3.3.1) that guides model to generate high-fidelity visual details after a series of denoising steps, and (2) training the diffusion model (§3.3.2) to correctly predict the noise that should be removed to restore the frame in each step.

3.3.1 Distortion-aware Conditioning

Similar to latest conditioned generative models, we need a conditioning signal c to guide the decoder: *generating what kind of frames can minimize the fidelity gap from the original frames?* Generally, the fidelity gap can be reflected by the *Fréchet Inception Distance* (FID) score [16], which is the most critical metric to measure the quality of images created by a generative model. To optimize the FID score, the decoder should be aware of the frame distortion caused by the encoder. As the decoder is empowered by a diffusion model, we need to embed the frame distortion into conditioning signal so that the model can correctly learn the conditional probability to generate high-fidelity frames like the realistic ones. Recall that CaDM's encoder introduces resolution downscaling and color bit-depth quantization to achieve a great compression ratio on video bitrate. The distortion is dominated by this resolution-color compression. Note that our CaDM still employs the standard H.264 protocol to package all the frames as bitstreams and does not modify the underlying streaming infrastructure. As low-quality videos are received by the ingest server, the decoder can capture all the compressed frames and upscale them to original resolution by using the fast bilinear interpolation. Following the mainstream mechanism to handle the conditioning [43], the decoder initializes a Gaussian noise as the generative seed and concatenates the upscaled frames with it along the channel dimension. The diffusion model takes the concatenation result to generate high-quality frames.

3.3.2 Model Training for Frame Restoration

Based on the discussion of embedding conditioning signals, the next step is to train the diffusion model for frame

restoration. The training procedure contains two stages: (1) forward diffusion and (2) reverse diffusion. Here, we present the most crucial formulations of these two stages.

Forward diffusion. Given the original data distribution of the frames that $\mathbf{x} \sim q(\mathbf{x})$, the forward stage aims at gradually degrading the frame quality by inserting a small amount of Gaussian noise $\epsilon \sim \mathcal{N}(0, \mathbf{I})$ into the frame through T steps. Based on the original frame \mathbf{x}_0 at the beginning, the core formulation of degraded frame \mathbf{x}_t in the t -th step ($t \in [1, T]$) can be described as:

$$\mathbf{x}_t = \sqrt{\alpha_t} \mathbf{x}_{t-1} + \sqrt{1 - \alpha_t} \epsilon_{t-1}, \quad (4)$$

where the hyper-parameter $0 < \alpha_t < 1$ controls the variance of the noise inserted in each step. Therefore, the frame \mathbf{x}_T will entirely lose the visual features after T steps. When $T \rightarrow +\infty$, \mathbf{x}_T is equivalent to an isotropic Gaussian distribution. Accumulating all the T steps, we can obtain the final degraded frame \mathbf{x}_T as:

$$\mathbf{x}_T = \sqrt{\bar{\alpha}_T} \mathbf{x}_0 + \sqrt{1 - \bar{\alpha}_T} \epsilon, \quad (5)$$

where $\bar{\alpha}_T = \prod_{t=1}^T \alpha_t$. Thus, we can formulate the final status of the forward diffusion as:

$$q(\mathbf{x}_T | \mathbf{x}_0) = \mathcal{N}(\mathbf{x}_T; \sqrt{\bar{\alpha}_T} \mathbf{x}_0, (1 - \bar{\alpha}_T) \mathbf{I}). \quad (6)$$

Briefly, the forward diffusion will gradually insert Gaussian noise into all the frames and finally make them equivalent to an isotropic Gaussian distribution.

Reverse diffusion. As to the frame restoration, we need to reverse the forward process of the diffusion model. This procedure is the major learning objective of our CaDM, which can be formulated as:

$$q(\mathbf{x}_{t-1} | \mathbf{x}_t, \mathbf{x}_0) = q(\mathbf{x}_t | \mathbf{x}_{t-1}, \mathbf{x}_0) \frac{q(\mathbf{x}_{t-1} | \mathbf{x}_0)}{q(\mathbf{x}_t | \mathbf{x}_0)}. \quad (7)$$

Therefore, we can train the diffusion model θ to learn this probability by minimizing the gap between the predicted noise ϵ_θ and true noise ϵ_t added in the t -th step during forward stage. Following this principle, we can formulate the corresponding loss function \mathcal{L} as:

$$\begin{aligned} \mathcal{L} &= \mathbb{E}_{t \sim [1, T], \mathbf{x}_0, \epsilon_t} [\|\epsilon_t - \epsilon_\theta(\mathbf{x}_t, t, c)\|^2] \\ &= \sum_{t=1}^T \mathbb{E}_{\mathbf{x}_0, \epsilon_t} [\|\epsilon_t - \epsilon_\theta(\sqrt{\alpha_t} \mathbf{x}_0 + \sqrt{1 - \alpha_t} \epsilon_t, t, c)\|^2], \quad (8) \end{aligned}$$

where t is the denoising level reflected by the step index, \mathbf{x}_t is the restored sample in step t , and c is the distortion-aware conditions of low-quality video frames. By feeding these variables into the diffusion model θ , we can optimize CaDM to hold sufficient restoration capacity to generate high-fidelity videos from the compressed bitstreams. In summary, the training procedure to generate the diffusion model and inference procedure to restore frame quality are summarized in Algorithm 1 and Algorithm 2, respectively.

Algorithm 1 Training diffusion model θ until convergence

Input: original frames \mathbf{x} , scaling factor s , bit-depth n .

Output: converged model θ .

- 1: $\hat{\mathbf{x}} = \text{Encode}(\mathbf{x}; s, n)$; ▷ Get the compressed frames.
 - 2: **repeat**
 - 3: $c \leftarrow \text{Upscale}(\hat{\mathbf{x}})$; ▷ Fast bilinear interpolation.
 - 4: $t \sim \text{Uniform}(1, \dots, T)$;
 - 5: $\epsilon \sim \mathcal{N}(\mathbf{0}, \mathbf{I})$; ▷ Gaussian noise.
 - 6: Take gradient descent step on:
 - 7: $\nabla_\theta \|\epsilon_t - \epsilon_\theta(\sqrt{\alpha_t} \mathbf{x} + \sqrt{1 - \alpha_t} \epsilon_t, t, c)\|^2$;
 - 8: **until** θ is converged; ▷ End with a converged model.
-

Algorithm 2 Inference in T steps for frame restoration

Input: compressed frames $\hat{\mathbf{x}}$, pre-trained model θ .

Output: restored frames $\tilde{\mathbf{x}}$.

- 1: $\mathbf{x}_T \sim \mathcal{N}(\mathbf{0}, \mathbf{I})$;
 - 2: $c \leftarrow \text{Upscale}(\hat{\mathbf{x}})$; ▷ Fast bilinear interpolation.
 - 3: **for** $t \in T, \dots, 1$ **do**
 - 4: $\mathbf{z} \sim \mathcal{N}(\mathbf{0}, \mathbf{I})$; ▷ Gaussian seed.
 - 5: $\Delta \mathbf{x}_0 \leftarrow \frac{\sqrt{\alpha_{t-1}} \mathbf{x}_t - \sqrt{1 - \alpha_t} \epsilon_\theta(\mathbf{x}_t, t, c)}{\sqrt{\alpha_t}}$;
 - 6: $\Delta \mathbf{x}_t \leftarrow \sqrt{1 - \bar{\alpha}_{t-1} - \sigma_t^2} \epsilon_\theta(\mathbf{x}_t, t, c)$;
 - 7: $\sigma_t^2 \leftarrow \frac{1 - \bar{\alpha}_{t-1}}{1 - \bar{\alpha}_t} \frac{1 - \alpha_t}{\alpha_{t-1}}$;
 - 8: $\mathbf{x}_{t-1} \leftarrow \Delta \mathbf{x}_0 + \Delta \mathbf{x}_t + \sigma_t \mathbf{z}$;
 - 9: **end for** ▷ End loop with \mathbf{x}_0 .
 - 10: $\tilde{\mathbf{x}} \leftarrow \mathbf{x}_{t-1}$;
 - 11: **Return** $\tilde{\mathbf{x}}$;
-

4. Evaluation

4.1. Experimental Setups

Benchmarks and Baselines. To match the runtime environment of realistic NVS pipelines, we evaluate CaDM with the modern OpenMMLab [39] benchmark and handle the video streaming by the widely-used H.264 [15] standard. We consider seven typical SR baselines with diverse model architectures, including SOTA BasicVSR++ [4], RealBasicVSR [5], IconVSR [3], MSRResNet [70], ESRGAN [53], EDSR [27], and SRCNN [12]. Following previous works [3–5], we use Vimeo-90K [57] as the training set, and use UDM10 [64] and Vid4 [28] as test sets. We conduct resolution-color compression (§3.2) to obtain low-quality videos, which are used for streaming delivery and video restoration. The seven baselines and CaDM are pre-trained based on the low-quality videos and original ones (serve as the ground-truth) to optimize the restoration capacity.

Performance measurement. As to encoder’s compression efficiency, we inspect how CaDM reduces the video delivery bitrates (Kbps), which is directly proportional to the size of streaming traffic. Also, as to decoder’s restoration performance, we calculate the *Fréchet Inception Distance*

Model	UDM10 [64]				Vid4 [28]			
	FID ↓	IS ↑	SSIM ↑	PSNR ↑	FID ↓	IS ↑	SSIM ↑	PSNR ↑
BasicVSR++ [4]	3.91	3.07±0.49	0.76	31.91	8.28	1.21±0.06	0.42	26.12
RealBasicVSR [5]	3.43	3.07±0.72	0.78	32.29	5.78	1.19±0.05	0.75	28.34
IconVSR [3]	2.89	3.10±0.40	0.81	32.53	5.32	1.20±0.06	0.74	28.39
MSRResNet [70]	4.17	3.04±0.42	0.77	31.92	10.04	1.20±0.07	0.69	28.03
ESRGAN [53]	4.73	2.99±0.67	0.75	31.53	18.48	1.14±0.04	0.58	27.43
EDSR [27]	3.73	2.92±0.45	0.75	31.56	12.29	1.10±0.03	0.62	27.66
SRCNN [12]	6.84	2.89±0.56	0.70	31.08	22.34	1.10±0.04	0.58	27.40
CaDM (Ours)	0.61	3.12±0.22	0.86	32.32	1.97	1.23±0.05	0.82	29.19

Table 1. Comparison with SOTA neural-enhancing methods, where the **red** and **blue** colors indicate the best and second-best performance, respectively. The videos are compressed with $4\times$ scaling factor and 4-bit color space, *i.e.*, holding 1/96 bitrate as vanilla H.264.

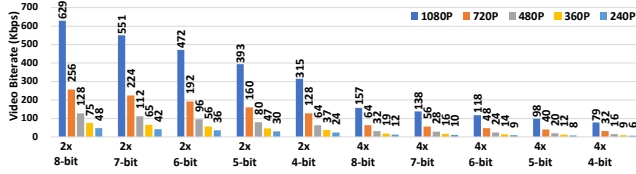


Figure 4. Video bitrates (Kbps) using different resolution-color settings. Bitrates of 1080P, 720P, 480P, 360P, and 240P achieved by vanilla H.264 are 7552, 3072, 1536, 896 and 576, respectively.

(FID) [16], Inception Score (IS) [44], Structural Similarity Index Method (SSIM) [54] and Peak Signal-to-noise Ratio (PSNR) [18] between the restored videos and the original ones. FID is the lower the better, while IS, SSIM and PSNR are the opposite. These are modern quality assessment metrics used by latest neural-enhancing works [34,42,43,49,50]. We also compare CaDM’s *rate-distortion* trade-off between streaming bitrate saving and video quality restoration with the baselines. Ablation studies of resolution scaling factor, color bit-depth, and H.264 configuration are also discussed. Due to the page limit, we present the most essential results here. More detailed analysis and visualization can be found in the supplementary materials.

4.2. End-to-end Performance

4.2.1 Inspection of Bitrate Saving

Saving video bitrate is the first objective of an efficient NVS paradigm. As shown in Figure 4, we compare CaDM’s encoder efficiency with vanilla H.264 and inspect the video bitrates (Kbps) under different resolution-color settings. The resolution scaling factor is set from $2\times$ to $4\times$, which are suitable to downscale common 1080P and 720P videos. Also, original video frames are represented in 24-bit color space while CaDM restricts the color bit-depth in [4, 8]. All the videos are encoded as 30 frames per second. It is clear that CaDM yields much lower video bitrate over the vanilla H.264. By using a larger scaling factor and lower color bit-depth (*e.g.*, $4\times$, 4-bit), CaDM finally achieves a near $100\times$ bitrate reduction. This makes CaDM qualified to deliver high-definition 1080P video streaming on the ingest side.

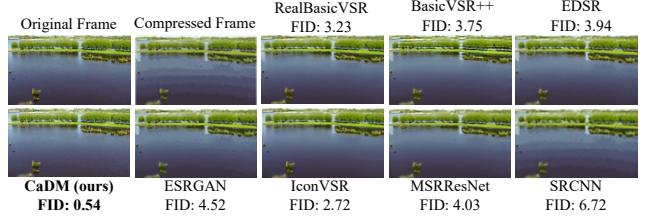


Figure 5. Visualization of restoration performance by using different methods. Only CaDM can recover high-fidelity visual details as the original frame. Please zoom in for best illustration.

4.2.2 Inspection of Restoration Quality

Apart from bitrate saving, providing high restoration quality is another key objective. As shown in Table 1, we compare CaDM’s restoration performance with the seven baselines. We can observe that CaDM significantly outperforms them in terms of FID, IS and SSIM. Here, the FID is the most crucial metric to compare the distribution between restored frames and the original ones, providing more precise measurement over the earlier IS score. Meanwhile, SSIM is a widely-adopted metric to reflect the perceptual similarity between two frames, especially for image enhancement. The highest scores of FID, IS and SSIM achieved by CaDM guarantee the excellent restoration quality for human vision, which is illustrated by the case in Figure 5. Note that CaDM does not always achieve the highest PSNR because the generative procedure inside CaDM’s diffusion model inserts a series of Gaussian noise to recover the visual details, which enlarges the L2 distance in PSNR. Previous works have verified that PSNR does not necessarily match the perceptual image quality [2,7,52]. Therefore, we mainly focus on FID, IS and SSIM to evaluate the restoration quality.

4.2.3 Inspection of Rate-distortion Trade-off

We inspect the *rate-distortion* trade-off between video bitrate and restoration quality, when using CaDM and the seven baselines. The bitrate is adjusted by changing the resolution scaling factor and color bit-depth. The baseline comparison can be best understood by checking Figure 6,

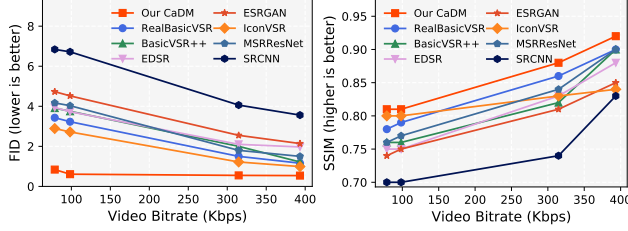


Figure 6. Comparison of the restoration quality under different bitrates, where CaDM consistently outperforms existing methods.

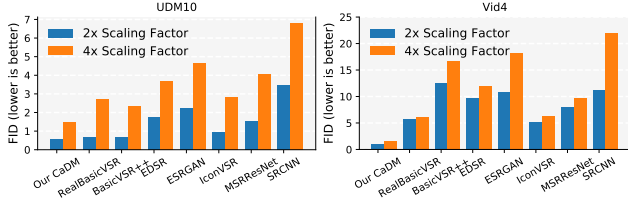


Figure 7. Restoration quality under different frame resolutions.

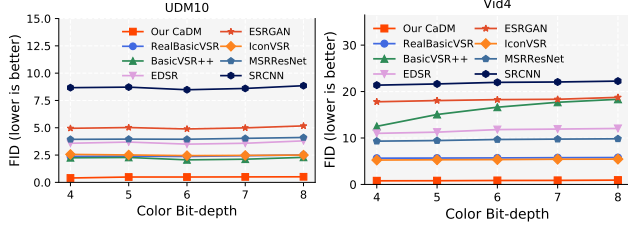


Figure 8. Restoration quality under different color bit-depth.

which reports the restoration scores under different video bitrates. We can observe that a higher bitrate brings a better restoration quality, where CaDM significantly outperforms other baselines. This comparison explicitly demonstrates CaDM’s superiority in bitrate saving and video restoration.

4.3. Ablation Studies

4.3.1 Effect of Resolution Scaling Factor

We inspect how resolution scaling factor impacts DaCM’s restoration performance. A larger factor will compress more visual information on original frames and make the restoration procedure harder, thus leading to a worse FID score. As shown in Figure 7, our CaDM significantly outperforms the baselines with much better FID scores under different scaling factors. This verifies that CaDM is qualified to deliver commodity 1080P/720P streaming in low-resolution versions while not incurring quality degradation.

4.3.2 Effect of Color Bit-depth

Recall that color bit-depth also directly impacts the restoration performance. We compare CaDM with the baselines by using different bit-depths, ranging from 4 to 8. A lower bit-depth will reduce the color number and lose more distribution information of pixel values, thus also yielding a harder restoration task. Comparison results in Figure 8 show that

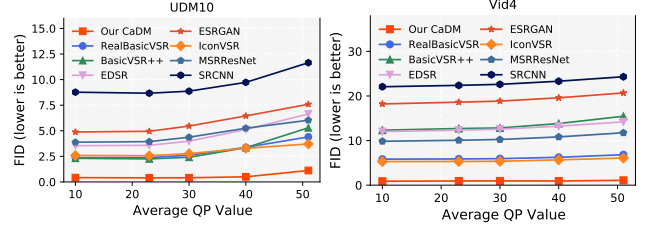


Figure 9. Restoration quality under different H.264 QP settings.

our CaDM consistently achieves the best restoration scores, verifying its powerful synthesis capacity to generate high-fidelity visual details, even in extreme low color space.

4.3.3 Effect of H.264 Configuration

As an NVS paradigm, CaDM is established based on the standard H.264 protocol, where the setting of H.264 also impacts CaDM’s restoration performance. Actually, H.264 conducts spatial-temporal compression through the macroblock-wise bit allocation, which is a kind of data quantization and is controlled by the *Quantization Parameter* (QP) [46]. In the 24-bit color space, QP ranges from 0 to 51. Given a frame, the lower the average QP is, the more bits will be allocated to it, thus with better visual quality. However, a lower QP value will also lead to a larger video bitrate. Therefore, we mainly focus on the impacts from H.264’s QP setting. As shown in Figure 9, a higher QP will make H.264 lose more visual information and lead to a worse restoration quality. However, our CaDM consistently outperforms all the baselines with much better FID scores and lower sensitivity to QP degradation. This verifies CaDM is compatible with the commodity H.264 codecs.

5. Conclusion

Video streaming is a significant infrastructure to deliver multimedia content and deploy perception services across the Internet. We identify the performance bottleneck on the ingest side and develop new insights into designing efficient NVS frameworks. Aiming at improving the *rate-distortion* trade-off between bitrate saving and quality restoration, we conduct an encoder-decoder synergy and propose the *Codec-aware Diffusion Modeling* (CaDM), a novel NVS paradigm to significantly reduce the streaming delivery bitrate while guaranteeing perfect restoration quality on the compressed videos. First, CaDM introduces the resolution-color compression to make the encoder fit streamer’s uplink environment. Second, CaDM optimizes the decoder’s enhancement capacity by leveraging the visual-synthesis genius of diffusion models. Evaluations based on public cloud services verify that CaDM effectively achieves an order of magnitude improvement in bitrate saving and holds the state-of-the-art restoration performance in different quality assessment metrics.

References

- [1] Athula Balachandran, Vyas Sekar, Aditya Akella, Srinivasan Seshan, Ion Stoica, and Hui Zhang. Developing a predictive model of quality of experience for internet video. In Dah Ming Chiu, Jia Wang, Paul Barford, and Srinivasan Seshan, editors, *Proceedings of the Annual conference of the ACM Special Interest Group on Data Communication on the applications, technologies, architectures, and protocols for computer communication (SIGCOMM)*, pages 339–350. ACM, 2013. 1
- [2] Yochai Blau and Tomer Michaeli. The perception-distortion tradeoff. In *Proceedings of the IEEE Conference on Computer Vision and Pattern Recognition (CVPR)*, pages 6228–6237. Computer Vision Foundation / IEEE Computer Society, 2018. 7
- [3] Kelvin C. K. Chan, Xintao Wang, Ke Yu, Chao Dong, and Chen Change Loy. Basicvsr: The search for essential components in video super-resolution and beyond. In *Proceedings of the IEEE Conference on Computer Vision and Pattern Recognition (CVPR)*, pages 4947–4956. Computer Vision Foundation / IEEE, 2021. 3, 6, 7
- [4] Kelvin C. K. Chan, Shangchen Zhou, Xiangyu Xu, and Chen Change Loy. Basicvsr++: Improving video super-resolution with enhanced propagation and alignment. In *Proceedings of the IEEE/CVF Conference on Computer Vision and Pattern Recognition (CVPR)*, pages 5962–5971. IEEE, 2022. 2, 3, 6, 7
- [5] Kelvin C. K. Chan, Shangchen Zhou, Xiangyu Xu, and Chen Change Loy. Investigating tradeoffs in real-world video super-resolution. In *Proceedings of the IEEE/CVF Conference on Computer Vision and Pattern Recognition (CVPR)*, pages 5952–5961. IEEE, 2022. 3, 6, 7
- [6] Jun-Ho Choi, Jun-Hyuk Kim, Manri Cheon, and Jong-Seok Lee. Deep learning-based image super-resolution considering quantitative and perceptual quality. *Neurocomputing*, 398:347–359, 2020. 3
- [7] Jun-Ho Choi, Huan Zhang, Jun-Hyuk Kim, Cho-Jui Hsieh, and Jong-Seok Lee. Evaluating robustness of deep image super-resolution against adversarial attacks. In *Proceedings of the IEEE/CVF International Conference on Computer Vision (ICCV)*, pages 303–311. IEEE, 2019. 7
- [8] Mengyu Chu, You Xie, Jonas Mayer, Laura Leal-Taixé, and Nils Thuerey. Learning temporal coherence via self-supervision for gan-based video generation. *ACM Trans. Graph.*, 39(4):75, 2020. 3
- [9] Mallesham Dasari, Kumara Kahatapitiya, Samir R. Das, Aruna Balasubramanian, and Dimitris Samaras. Swift: Adaptive video streaming with layered neural codecs. In Amar Phanishayee and Vyas Sekar, editors, *Proceedings of the USENIX Symposium on Networked Systems Design and Implementation (NSDI)*, pages 103–118. USENIX Association, 2022. 1, 2, 3, 4
- [10] Dandan Ding, Zhan Ma, Di Chen, Qingshuang Chen, Zoe Liu, and Fengqing Zhu. Advances in video compression system using deep neural network: A review and case studies. *Proc. IEEE*, 109(9):1494–1520, 2021. 1
- [11] Florin Dobrian, Vyas Sekar, Asad Awan, Ion Stoica, Dilip Antony Joseph, Aditya Ganjam, Jibin Zhan, and Hui Zhang. Understanding the impact of video quality on user engagement. In Srinivasan Keshav, Jörg Liebeherr, John W. Byers, and Jeffrey C. Mogul, editors, *Proceedings of the Annual conference of the ACM Special Interest Group on Data Communication on the applications, technologies, architectures, and protocols for computer communication (SIGCOMM)*, pages 362–373. ACM, 2011. 1
- [12] Chao Dong, Chen Change Loy, Kaiming He, and Xiaoou Tang. Image super-resolution using deep convolutional networks. *IEEE Trans. Pattern Anal. Mach. Intell.*, 38(2):295–307, 2016. 6, 7
- [13] Kuntai Du, Ahsan Pervaiz, Xin Yuan, Aakanksha Chowdhery, Qizheng Zhang, Henry Hoffmann, and Junchen Jiang. Server-driven video streaming for deep learning inference. In Henning Schulzrinne and Vishal Misra, editors, *Proceedings of the Annual conference of the ACM Special Interest Group on Data Communication on the applications, technologies, architectures, and protocols for computer communication (SIGCOMM)*, pages 557–570. ACM, 2020. 1
- [14] Kuntai Du, Qizheng Zhang, Anton Arapin, Haodong Wang, Zhengxu Xia, and Junchen Jiang. Accmpeg: Optimizing video encoding for accurate video analytics. In Diana Marculescu, Yuejie Chi, and Carole-Jean Wu, editors, *Proceedings of the Machine Learning and Systems (MLSys)*. mlsys.org, 2022. 1, 2, 3
- [15] H.264. H.264 official website. <https://www.itu.int/rec/T-REC-H.264>, 2022. 2, 3, 6
- [16] Martin Heusel, Hubert Ramsauer, Thomas Unterthiner, Bernhard Nessler, and Sepp Hochreiter. Gans trained by a two time-scale update rule converge to a local nash equilibrium. In Isabelle Guyon, Ulrike von Luxburg, Samy Bengio, Hanna M. Wallach, Rob Fergus, S. V. N. Vishwanathan, and Roman Garnett, editors, *Proceedings of the Annual Conference on Neural Information Processing Systems (NeurIPS)*, pages 6626–6637, 2017. 5, 7
- [17] Jonathan Ho, Ajay Jain, and Pieter Abbeel. Denoising diffusion probabilistic models. In Hugo Larochelle, Marc’Aurelio Ranzato, Raia Hadsell, Maria-Florina Balcan, and Hsuan-Tien Lin, editors, *Proceedings of the Annual Conference on Neural Information Processing Systems (NeurIPS)*, 2020. 3
- [18] Alain Horé and Djemel Ziou. Image quality metrics: PSNR vs. SSIM. In *Proceedings of the International Conference on Pattern Recognition (ICPR)*, pages 2366–2369. IEEE Computer Society, 2010. 7
- [19] Randell Jesup, Salvatore Loreto, and Michael Tüxen. Webrtc data channel establishment protocol. *RFC*, 8832:1–12, 2021. 1
- [20] Xue Jiang, Xiulian Peng, Chengyu Zheng, Huaying Xue, Yuan Zhang, and Yan Lu. End-to-end neural speech coding for real-time communications. In *Proceedings of the IEEE International Conference on Acoustics, Speech and Signal Processing (ICASSP)*, pages 866–870. IEEE, 2022. 1
- [21] Justin Johnson, Alexandre Alahi, and Li Fei-Fei. Perceptual losses for real-time style transfer and super-resolution. In Bastian Leibe, Jiri Matas, Nicu Sebe, and Max Welling, editors, *Proceedings of the European Conference on Computer*

- Vision (ECCV)*, volume 9906 of *Lecture Notes in Computer Science*, pages 694–711. Springer, 2016. 1
- [22] Jaehong Kim, Youngmok Jung, Hyunho Yeo, Juncheol Ye, and Dongsu Han. Neural-enhanced live streaming: Improving live video ingest via online learning. In Henning Schulzrinne and Vishal Misra, editors, *Proceedings of the Annual conference of the ACM Special Interest Group on Data Communication on the applications, technologies, architectures, and protocols for computer communication (SIGCOMM)*, pages 107–125. ACM, 2020. 1, 2, 3, 4
- [23] Jiwon Kim, Jung Kwon Lee, and Kyoung Mu Lee. Accurate image super-resolution using very deep convolutional networks. In *Proceedings of the IEEE Conference on Computer Vision and Pattern Recognition (CVPR)*, pages 1646–1654. IEEE Computer Society, 2016. 1
- [24] Jonathan Lennox, Kevin Gross, Suhas Nandakumar, Gonzalo Salgueiro, and Bo Burman. A taxonomy of semantics and mechanisms for real-time transport protocol (rtp) sources. *RFC*, 7656:1–46, 2015. 1
- [25] Jiahao Li, Bin Li, and Yan Lu. Deep contextual video compression. In Marc’Aurelio Ranzato, Alina Beygelzimer, Yann N. Dauphin, Percy Liang, and Jennifer Wortman Vaughan, editors, *Proceedings of the Annual Conference on Neural Information Processing Systems (NeurIPS)*, pages 18114–18125, 2021. 1
- [26] Tong Li, Kai Zheng, Ke Xu, Rahul Arvind Jadhav, Tao Xiong, Keith Winstein, and Kun Tan. TACK: improving wireless transport performance by taming acknowledgments. In Henning Schulzrinne and Vishal Misra, editors, *Proceedings of the Annual conference of the ACM Special Interest Group on Data Communication on the applications, technologies, architectures, and protocols for computer communication (SIGCOMM)*, pages 15–30. ACM, 2020. 1
- [27] Bee Lim, Sanghyun Son, Heewon Kim, Seungjun Nah, and Kyoung Mu Lee. Enhanced deep residual networks for single image super-resolution. In *Proceedings of the IEEE Conference on Computer Vision and Pattern Recognition (CVPR)*, pages 1132–1140. IEEE Computer Society, 2017. 1, 3, 6, 7
- [28] Ce Liu and Deqing Sun. On bayesian adaptive video super resolution. *IEEE Trans. Pattern Anal. Mach. Intell.*, 36(2):346–360, 2014. 6, 7
- [29] Dong Liu, Yue Li, Jianping Lin, Houqiang Li, and Feng Wu. Deep learning-based video coding: A review and a case study. *ACM Comput. Surv.*, 53(1):11:1–11:35, 2020. 1
- [30] Jing Liu, Pingping Liu, Yuting Su, Peiguang Jing, and Xiaokang Yang. Spatiotemporal symmetric convolutional neural network for video bit-depth enhancement. *IEEE Trans. Multimed.*, 21(9):2397–2406, 2019. 1, 4
- [31] Jiaming Liu, Ming Lu, Kaixin Chen, Xiaoqi Li, Shizun Wang, Zhaoqing Wang, Enhua Wu, Yurong Chen, Chuang Zhang, and Ming Wu. Overfitting the data: Compact neural video delivery via content-aware feature modulation. In *Proceedings of the IEEE/CVF International Conference on Computer Vision (ICCV)*, pages 4611–4620. IEEE, 2021. 1, 2
- [32] Jing Liu, Ziwen Yang, Yuting Su, and Xiaokang Yang. Tanet: Target attention network for video bit-depth enhancement. *IEEE Trans. Multimed.*, 24:4212–4223, 2022. 1, 4
- [33] Guo Lu, Wanli Ouyang, Dong Xu, Xiaoyun Zhang, Chunlei Cai, and Zhiyong Gao. DVC: an end-to-end deep video compression framework. In *Proceedings of the IEEE Conference on Computer Vision and Pattern Recognition (CVPR)*, pages 11006–11015. Computer Vision Foundation / IEEE, 2019. 1
- [34] Andreas Lugmayr, Martin Danelljan, Andrés Romero, Fisher Yu, Radu Timofte, and Luc Van Gool. Repaint: Inpainting using denoising diffusion probabilistic models. In *Proceedings of the IEEE/CVF Conference on Computer Vision and Pattern Recognition (CVPR)*, pages 11451–11461. IEEE, 2022. 3, 7
- [35] Di Ma, Fan Zhang, and David R. Bull. Gan-based effective bit depth adaptation for perceptual video compression. In *Proceedings of the IEEE International Conference on Multimedia and Expo (ICME)*, pages 1–6. IEEE, 2020. 1
- [36] Sachit Menon, Alexandru Damian, Shijia Hu, Nikhil Ravi, and Cynthia Rudin. PULSE: self-supervised photo upsampling via latent space exploration of generative models. In *Proceedings of the IEEE/CVF Conference on Computer Vision and Pattern Recognition (CVPR)*, pages 2434–2442. Computer Vision Foundation / IEEE, 2020. 3
- [37] Arvind Narayanan, Xumiao Zhang, Ruiyang Zhu, Ahmad Hassan, Shuwei Jin, Xiao Zhu, Xiaoxuan Zhang, Denis Rybkin, Zhengxuan Yang, Zhuoqing Morley Mao, Feng Qian, and Zhi-Li Zhang. A variegated look at 5g in the wild: performance, power, and qoe implications. In Fernando A. Kuipers and Matthew C. Caesar, editors, *Proceedings of the Annual conference of the ACM Special Interest Group on Data Communication on the applications, technologies, architectures, and protocols for computer communication (SIGCOMM)*, pages 610–625. ACM, 2021. 1
- [38] Minh Nguyen, Ekrem Çetinkaya, Hermann Hellwagner, and Christian Timmerer. Super-resolution based bitrate adaptation for HTTP adaptive streaming for mobile devices. In *Proceedings of the Mile-High Video Conference (MHV)*, pages 70–76. ACM, 2022. 1, 2, 3
- [39] OpenMMLab. Openmmlab dataset. <https://openmmlab.com/dataset>, 2022. 6
- [40] Mirko Palmer, Malte Appel, Kevin Spiteri, Balakrishnan Chandrasekaran, Anja Feldmann, and Ramesh K. Sitaraman. VOXEL: cross-layer optimization for video streaming with imperfect transmission. In Georg Carle and Jörg Ott, editors, *Proceedings of the International Conference on emerging Networking EXperiments and Technologies (CoNEXT)*, pages 359–374. ACM, 2021. 1
- [41] Yanyuan Qin, Shuai Hao, Krishna R. Pattipati, Feng Qian, Subhabrata Sen, Bing Wang, and Chaoqun Yue. ABR streaming of vbr-encoded videos: characterization, challenges, and solutions. In Xenofontas A. Dimitropoulos, Alberto Dainotti, Laurent Vanbever, and Theophilus Benson, editors, *Proceedings of the International Conference on emerging Networking EXperiments and Technologies (CoNEXT)*, pages 366–378. ACM, 2018. 1
- [42] Robin Rombach, Andreas Blattmann, Dominik Lorenz, Patrick Esser, and Björn Ommer. High-resolution image synthesis with latent diffusion models. In *Proceedings of the IEEE/CVF Conference on Computer Vision and Pattern Recognition (CVPR)*, pages 10674–10685. IEEE, 2022. 3, 7

- [43] Chitwan Saharia, Jonathan Ho, William Chan, Tim Salimans, David J. Fleet, and Mohammad Norouzi. Image super-resolution via iterative refinement. *arXiv preprint*, abs/2104.07636, 2021. 3, 5, 7
- [44] Tim Salimans, Ian J. Goodfellow, Wojciech Zaremba, Vicki Cheung, Alec Radford, and Xi Chen. Improved techniques for training gans. In Daniel D. Lee, Masashi Sugiyama, Ulrike von Luxburg, Isabelle Guyon, and Roman Garnett, editors, *Proceedings of the Annual Conference on Neural Information Processing Systems (NeurIPS)*, pages 2226–2234, 2016. 7
- [45] Henning Schulzrinne, Stephen L. Casner, Ron Frederick, and Van Jacobson. Rtp: A transport protocol for real-time applications. *RFC*, 1889:1–75, 1996. 1
- [46] Heiko Schwarz, Detlev Marpe, and Thomas Wiegand. Overview of the scalable video coding extension of the H.264/AVC standard. *IEEE Trans. Circuits Syst. Video Technol.*, 17(9):1103–1120, 2007. 8
- [47] Kalpathy Sivaraman and G. Kavitha. Real-time streaming protocol (rtsp). *Eurasian Journal of Analytical Chemistry*, 13:705–709, 2019. 1
- [48] Jae Woong Soh, Gu Yong Park, Junho Jo, and Nam Ik Cho. Natural and realistic single image super-resolution with explicit natural manifold discrimination. In *Proceedings of the IEEE Conference on Computer Vision and Pattern Recognition (CVPR)*, pages 8122–8131. Computer Vision Foundation / IEEE, 2019. 3
- [49] Jiaming Song, Chenlin Meng, and Stefano Ermon. Denoising diffusion implicit models. In *Proceedings of the International Conference on Learning Representations (ICLR)*. OpenReview.net, 2021. 3, 7
- [50] Yang Song, Jascha Sohl-Dickstein, Diederik P. Kingma, Abhishek Kumar, Stefano Ermon, and Ben Poole. Score-based generative modeling through stochastic differential equations. In *Proceedings of the International Conference on Learning Representations (ICLR)*. OpenReview.net, 2021. 3, 7
- [51] Bo Wang, Mingwei Xu, Fengyuan Ren, Chao Zhou, and Jianping Wu. Cratus: A lightweight and robust approach for mobile live streaming. *IEEE Trans. Mob. Comput.*, 21(8):2761–2775, 2022. 1
- [52] Xintao Wang, Liangbin Xie, Chao Dong, and Ying Shan. Real-esrgan: Training real-world blind super-resolution with pure synthetic data. In *Proceedings of the IEEE/CVF International Conference on Computer Vision (ICCV)*, pages 1905–1914. IEEE, 2021. 3, 7
- [53] Xintao Wang, Ke Yu, Shixiang Wu, Jinjin Gu, Yihao Liu, Chao Dong, Yu Qiao, and Chen Change Loy. ESRGAN: enhanced super-resolution generative adversarial networks. In Laura Leal-Taixé and Stefan Roth, editors, *Proceedings of the European Conference on Computer Vision (ECCV)*, volume 11133 of *Lecture Notes in Computer Science*, pages 63–79. Springer, 2018. 6, 7
- [54] Zhou Wang, Alan C. Bovik, Hamid R. Sheikh, and Eero P. Simoncelli. Image quality assessment: from error visibility to structural similarity. *IEEE Trans. Image Process.*, 13(4):600–612, 2004. 7
- [55] Zelong Wang, Zhenxiao Luo, Miao Hu, Di Wu, Youlong Cao, and Yi Qin. Revisiting super-resolution for internet video streaming. In *Proceedings of the 32nd Workshop on Network and Operating Systems Support for Digital Audio and Video (NOSSDAV)*, 2022. 2
- [56] Shichang Xu, Subhabrata Sen, and Z. Morley Mao. CSI: inferring mobile ABR video adaptation behavior under HTTPS and QUIC. In Angelos Bilas, Kostas Magoutis, Evangelos P. Markatos, Dejan Kostic, and Margo I. Seltzer, editors, *Proceedings of the European Conference on Computer Systems (EuroSys)*, pages 33:1–33:16. ACM, 2020. 1
- [57] Tianfan Xue, Baian Chen, Jiajun Wu, Donglai Wei, and William T. Freeman. Video enhancement with task-oriented flow. *Int. J. Comput. Vis.*, 127(8):1106–1125, 2019. 6
- [58] Francis Y. Yan, Hudson Ayers, Chenzhi Zhu, Sadjad Fouladi, James Hong, Keyi Zhang, Philip Alexander Levis, and Keith Winstein. Learning in situ: a randomized experiment in video streaming. In Ranjita Bhagwan and George Porter, editors, *Proceedings of the USENIX Symposium on Networked Systems Design and Implementation (NSDI)*, pages 495–511. USENIX Association, 2020. 1
- [59] Junyan Yang, Yang Jiang, and Shuoyao Wang. Enhancement or super-resolution: Learning-based adaptive video streaming with client-side video processing. *arXiv preprint*, abs/2201.08197, 2022. 3
- [60] Xinlei Yang, Hao Lin, Zhenhua Li, Feng Qian, Xingyao Li, Zhiming He, Xudong Wu, Xianlong Wang, Yunhao Liu, Zhi Liao, Daqiang Hu, and Tianyin Xu. Mobile access bandwidth in practice: measurement, analysis, and implications. In Fernando Kuipers and Ariel Orda, editors, *Proceedings of the Annual conference of the ACM Special Interest Group on Data Communication on the applications, technologies, architectures, and protocols for computer communication (SIGCOMM)*, pages 114–128. ACM, 2022. 1
- [61] Hyunho Yeo, Chan Ju Chong, Youngmok Jung, Juncheol Ye, and Dongsu Han. NEMO: enabling neural-enhanced video streaming on commodity mobile devices. In *Proceedings of the Annual International Conference on Mobile Computing and Networking (MobiCom)*, pages 28:1–28:14. ACM, 2020. 1, 2, 3, 4
- [62] Hyunho Yeo, Youngmok Jung, Jaehong Kim, Jinwoo Shin, and Dongsu Han. Neural adaptive content-aware internet video delivery. In Andrea C. Arpaci-Dusseau and Geoff Voelker, editors, *Proceedings of the USENIX Symposium on Operating Systems Design and Implementation (OSDI)*, pages 645–661. USENIX Association, 2018. 1, 3, 4
- [63] Hyunho Yeo, Hwijoon Lim, Jaehong Kim, Youngmok Jung, Juncheol Ye, and Dongsu Han. Neuroscaler: neural video enhancement at scale. In Fernando Kuipers and Ariel Orda, editors, *Proceedings of the Annual conference of the ACM Special Interest Group on Data Communication on the applications, technologies, architectures, and protocols for computer communication (SIGCOMM)*, pages 795–811. ACM, 2022. 1, 2, 3, 4
- [64] Peng Yi, Zhongyuan Wang, Kui Jiang, Junjun Jiang, and Jiayi Ma. Progressive fusion video super-resolution network via exploiting non-local spatio-temporal correlations. In *Proceedings of the IEEE/CVF International Conference*

- on *Computer Vision (ICCV)*, pages 3106–3115. IEEE, 2019. 6, 7
- [65] Xiaoqi Yin, Abhishek Jindal, Vyas Sekar, and Bruno Sinopoli. A control-theoretic approach for dynamic adaptive video streaming over HTTP. In Steve Uhlig, Olaf Maennel, Brad Karp, and Jitendra Padhye, editors, *Proceedings of the Annual conference of the ACM Special Interest Group on Data Communication on the applications, technologies, architectures, and protocols for computer communication (SIGCOMM)*, pages 325–338. ACM, 2015. 1
- [66] YouTube. Youtube live streaming official website. <https://www.youtube.com/live>, 2022. 1, 2
- [67] Anlan Zhang, Chendong Wang, Bo Han, and Feng Qian. Efficient volumetric video streaming through super resolution. In *Proceedings of the International Workshop on Mobile Computing Systems and Applications (HotMobile)*, pages 106–111. ACM, 2021. 3
- [68] Anlan Zhang, Chendong Wang, Bo Han, and Feng Qian. Yuzu: Neural-enhanced volumetric video streaming. In Amar Phanishayee and Vyas Sekar, editors, *Proceedings of the USENIX Symposium on Networked Systems Design and Implementation (NSDI)*, pages 137–154. USENIX Association, 2022. 1, 2, 3
- [69] Fan Zhang, Mariana Afonso, and David R. Bull. Vistra2: Video coding using spatial resolution and effective bit depth adaptation. *Signal Process. Image Commun.*, 97:116355, 2021. 1
- [70] Kai Zhang, Martin Danelljan, Yawei Li, Radu Timofte, Jie Liu, Jie Tang, Gangshan Wu, Yu Zhu, Xiangyu He, Wenjie Xu, Chenghua Li, Cong Leng, Jian Cheng, Guangyang Wu, Wenyi Wang, Xiaohong Liu, Hengyuan Zhao, Xiangtao Kong, Jingwen He, Yu Qiao, Chao Dong, Xiaotong Luo, Liang Chen, Jiangtao Zhang, Maitreya Suin, Kuldeep Purohit, A. N. Rajagopalan, Xiaochuan Li, Zhiqiang Lang, Jiangtao Nie, Wei Wei, Lei Zhang, Abdul Muqet, Jiwon Hwang, Subin Yang, Jung Heum Kang, Sung-Ho Bae, Yongwoo Kim, Yanyun Qu, Geun-Woo Jeon, Jun-Ho Choi, Jun-Hyuk Kim, Jong-Seok Lee, Steven Marty, Éric Marty, Dongliang Xiong, Siang Chen, Lin Zha, Jiande Jiang, Xinbo Gao, Wen Lu, Haicheng Wang, Vineeth Bhaskara, Alex Levinstein, Stavros Tsogkas, Allan D. Jepson, Xiangzhen Kong, Tongtong Zhao, Shanshan Zhao, Hrishikesh P. S, Densen Puthussery, C. V. Jiji, Nan Nan, Shuai Liu, Jie Cai, Zibo Meng, Jiaming Ding, Chiu Man Ho, Xuehui Wang, Qiong Yan, Yuzhi Zhao, Long Chen, Long Sun, Wenhao Wang, Zhenbing Liu, Rushi Lan, Rao Muhammad Umer, and Christian Micheloni. AIM 2020 challenge on efficient super-resolution: Methods and results. In Adrien Bartoli and Andrea Fusiello, editors, *Proceedings of the European Conference on Computer Vision (ECCV)*, volume 12537 of *Lecture Notes in Computer Science*, pages 5–40. Springer, 2020. 6, 7
- [71] Yuanxing Zhang, Yushuo Guan, Kaigui Bian, Yunxin Liu, Hu Tuo, Lingyang Song, and Xiaoming Li. EPASS360: qoe-aware 360-degree video streaming over mobile devices. *IEEE Trans. Mob. Comput.*, 20(7):2338–2353, 2021. 1
- [72] Yulun Zhang, Yapeng Tian, Yu Kong, Bineng Zhong, and Yun Fu. Residual dense network for image super-resolution. In *Proceedings of the IEEE Conference on Computer Vision and Pattern Recognition (CVPR)*, pages 2472–2481. Computer Vision Foundation / IEEE Computer Society, 2018. 1
- [73] Zoom. Zoom meeting official website. <https://zoom.us/>, 2022. 1, 2